Journal on Oncology

www.journalononcology.org

Research Article

Open Access, Volume 2

The DECT Characteristics and Radiomics Model Predict the Infiltration of Lung Adenocarcinoma

Chuan Tian*

Department of Radiology, Kaiyuan People's Hospital, China.

Abstract

Objective: To explore the value of spectrum CT characteristics and imaging omics model to predict the infiltration of lung adenocarcinoma.

Materials and methods: Prospectively collected 196 patients who were treated from September 2019 to November 2020 in Kaiyuan People's Hospital, received unified standard dual energy CT scan, and postoperative pathology confirmed as early lung adenocarcinoma (pT1N0M0). The clinical characteristics and imaging characteristics of the patients were extracted, and three models were established: imaging omics model, mixed clinical manual imaging model and mixed model, and the diagnostic efficacy of the three models was compared by using the DeLong test.

Results: According to the pathological results, the patients were divided into pre-invasive lesion group and invasive lesion group; (1) The results of univariate analysis showed that gender, age, active smoking and whether the native place had a high incidence of lung cancer, the maximum diameter of lesions, plain scan CT value and enhanced arterial phase scanning, nodule type, nodule morphology and pleural traction depression were statistically significant between the two groups; Further post-multivariate analysis of nodule type, active smoking, pleural pulling and depression, and enhanced arterial phase scan 40 / 90 / 150keV single-energy imaging CT values were included in the mixed clinical manual imaging model, The AUC values of the model in the training and validation sets were 0.82 and 0.76, respectively; (2) Sixty-three imaging omics features were retained by univariate analysis, Through LASSO dimensionality reduction, 10 imaging omics characteristics were closely related to the infiltration of early lung adenocarcinoma, Five of these features were derived from the lesion itself, The other five features are derived from the peritumoral microenvironment; The AUC values of the imaging omics model in the training and validation sets were 0.86 and 0.87, respectively. (3) The AUC value of the mixed model in both the training set and the validation set was 0.88, and only the imaging omics score in the model was an independent predictor of early lung adenocarcinoma infiltration.

Conclusion: The imaging model based on energy spectrum CT has good prediction ability for early lung adenocarcinoma infiltration, and can provide reference for the selection of preoperative surgery in patients with early lung adenocarcinoma; the hybrid model of imaging model combined with clinical characteristics and manual imaging features has better prediction efficiency.

Keywords: Lung adenocarcinoma; Invasive; Imaging omics; Spectrum CT.

Manuscript Information: *Received: Oct 10, 2022; Accepted: Nov 14, 2022; Published: Nov 23, 2022*

Correspondance: *Chuan Tian, Department of Radiology, Kaiyuan People's Hospital, China.*

Tel: 15912158437; Email: 2672451163@qq.com

Citation: *Tian C. The DECT Characteristics and Radiomics Model Predict the Infiltration of Lung Adenocarcinoma J Oncology. 2022; 2(2): 1061.*

Copyright: © Tian C 2022. *Content published in the journal follows creative common attribution license.*

Preface

According to the global cancer statistics in 2021, lung cancer is among the top [1] in both morbidity and mortality. The WHO's latest 2021 lung tumor classification classifies adenocarcinoma in situ and atypical adenomaplasia as precursor lesions, and microinvasive adenocarcinoma and invasive adenocarcinoma are still classified as adenocarcinoma, which not only provides a basis for the conservative treatment of adenocarcinoma in situ, but also greatly reduces the psychological pressure of patients. At present, the treatment of early lung adenocarcinoma mainly adopts surgical resection, precursor lesions can take regular follow-up or elective surgery, take elective surgery of precursor lesions and microinvasive adenocarcinoma by sublobectomy can achieve a good prognosis, while invasive adenocarcinoma needs to take lobectomy or pulmonectomy to achieve a good prognosis. Therefore, it is crucial to accurately judge the grade of lesion invasion before surgery.

Materials and methods

Case collection

A prospective collection of 196 patients, including 196 lesions. Inclusion criteria: Patients with primary pulmonary nodules undergoing double-energy scanning.

Exclusion criteria are shown in **Figure 1.**

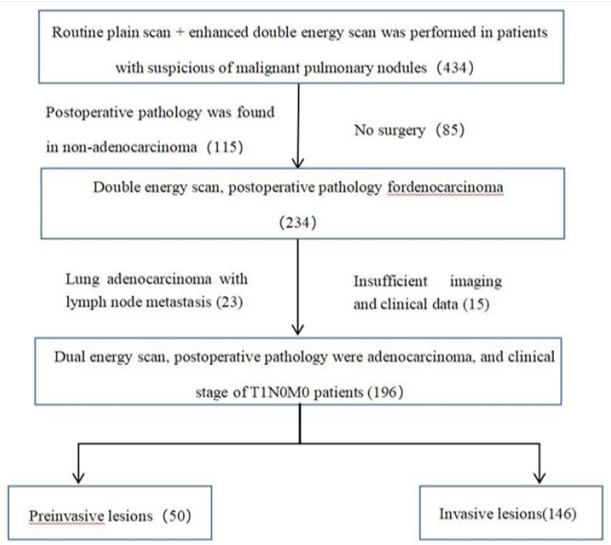

Figure 1: Exclusion criteria.

Feature extraction

The clinical characteristics and imaging characteristics of the included patients were extracted, including age, gender, current active smoking, whether their native place was Yunnan Xuanwei, and whether there were chest-related symptoms. Imaging features include: quantitative features (longest diameter of lesion, CT value of lesion flat scan, CT value of single energy image of enhanced arterial period) and qualitative features (nodule type, nodule morphology, burr features, clear tumor-lung interface, vacuolar features, air bronchial features, vascular tract features, and pleural depression features). Imaging omics features include the imaging omics features of nodules itself and imaging omics features within 5 mm range, the delineation of nodules itself as ROI 1, and then 5 mm range as ROI 2 (using semi-automatic software), extract the imaging omics features of the two regions of interest (Figure 2).

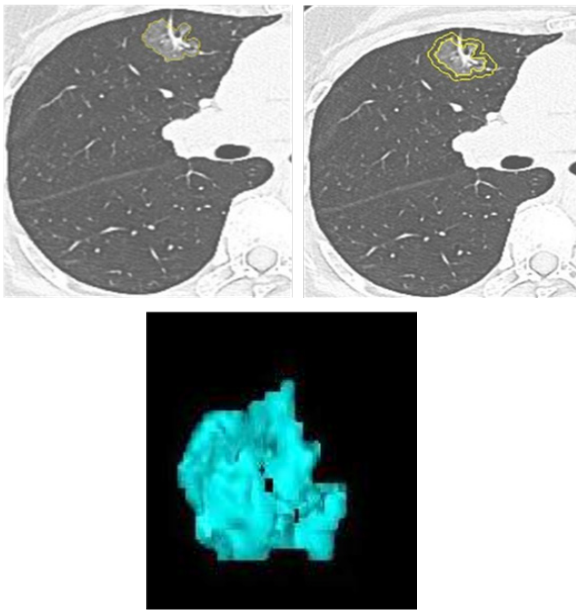

Figure 2: Image omics ROI delineation and feature extraction.

Model establishment

Manual imaging model established with patient clinical characteristics and manual imaging characteristics, combined with clinical characteristics and imaging omics characteristics, and mixed model established with clinical characteristics, manual imaging characteristics and imaging omics characteristics.

Statistical analysis

Statistical analysis of the collected data was performed using the statistical software R language. Chi-square test or Fisher exact test is used for statistical analysis for the counts data of the general clinical data and CT images, test for statistical normality of measurement data for the general clinical data and quantitative characteristics of CT images and use t-test for measurement data with normal distribution, otherwise, Mann-Whitney U test is used. LASSO regression and independent predictors, and DE LONG test was used to compare the diagnostic performance of the three models.

Results

Baseline characteristics

A total of 196 lesions were included in 196 patients in this study. The pathological results were: AAH 10, AAH with local AIS 7, AIS 11, MIA 3, AIS with MIA 15, AAH with local AIS with MIA 4, IA 146, IA in the invasive lesions, and the remaining lesions in the pre-invasive group. In this study, 84 males and 112 females had an age range of 34 – 81 years, with a mean age of 54.65 years. Pre-invasive and invasive lesions were divided into training and validation set in a ratio of 8:2. Statistically different characteristics of the training set and the validation sets are shown in Table 1 (see Appendix Table 1 for the full basic features).

Extract the features of the training set and analyze the data as follows

Clinical risk factor analysis results

Univariate analysis of the patients' general clinical data retained the characteristics of p <0.05, and the results are shown in Table 2.

Manual imaging feature analysis results

Univariate and multivariate regression analysis of traditional CT characteristics was retained at p<0.05. In the univariate analysis, as shown in Table 3 (see Appendix Table 2 for the full table) and Table 4, the nodule morphology, nodule type, pleural traction and depression showed statistical differences in the qualitative characteristics, such as the maximum diameter of the nodules and the lesion CT value.

Table 1: The distribution of statistically significant features in the training set and in the training set and validation set.

Characteristics	Overall cohort (*n* = 96)	Derivation Cohort (*n* = 158)	Validation Cohort (*n* = 38)	*P* Value
age	56.64 ± 9.91	54.83 ± 9.8	55.15 ± 10.82	0.001[a]
The longest diameter	1.83 ± 0.74	1.78 ± 0.76	1.86 ± 0.72	0.001[a]
Non-contrast CT value	-178.81 ± 66.60	-201.40 ± 74.78	-153.78 ± 53.24	0.001[a]

Table 2: Clinical characteristics Univariate analysis has statistically significant characteristics.

Clinical features		Preinvasive lesions	Invasive lesions	p
age		49.80 ± 9.12	56.41 ± 9.49	<0.001
sex	man	13	59	0.055
	female	27	59	
active smoking	yes	6	45	0.007
	no	34	73	
Xuanwei native place	yes	10	85	<0.001
	no	30	33	

Table 3: Statistically significant features in univariate analysis.

Qualitative characteristics		Preinvasive lesions	Invasive lesions	p
Nodular type	pGGN	19	15	<0.001
	mGGN	11	43	
	SN	10	60	
Nodular shape	round	19	22	0.001
	lobulated	11	55	
	Irregular	10	41	
Pleural traction and depression	yes	11	87	<0.001
	no	29	31	

Table 4: Characteristics of p <0.05 after univariate analysis of quantitative data in clinical and manual imaging characteristics.

Quantitative characteristics	Preinvasive lesions		Invasive lesions	test of normality p	Univariate analysis p
The longest diameter		1.27 ± 0.12	1.90 ± 0.08	0.003	<0.001
Non-contrast CT	value	-385.33 ± 58.00	-149.07 ± 25.81	0	<0.001
Single	40 keV	-270.48 ± 62.27	-38.80 ± 27.41	0	0.001
energy	70 keV	-366.61 ± 58.33	-127.38 ± 25.80	0	<0.001
spectrum in	90 keV	-398.50 ± 56.76	-152.86 ± 25.82	0	<0.001
arterial stage	110 keV	-413.19 ± 56.23	-169.25 ± 25.43	0	<0.001
CT value	150 keV	-408.09 ± 57.27	-180.16 ± 25.43	0	<0.001

Table 5: Clinical features, manual imaging features, and their coefficients of the included models after the LASSO multivariate regression analysis.

Features	Coefficients
Nodular type	0.612665616
active smoking	1.166783734
Pleural pull and depression	1.050779324
CT values of 90 keV single energy imaging for enhanced arterial phase scans	0.002036329
CT values of 40 keV single energy imaging for enhanced arterial phase scans	-0.000817706
CT values of 150 keV single energy imaging for enhanced arterial phase scans	-0.000127868

LASSO multivariate analysis of clinical features and manual imaging features in univariate analysis, as shown in Figure 3; 6 features closely related to the degree of early lung adenocarcinoma infiltration, including nodule type, active smoking, pleural pull and depression, and arterial single energy (40 / 90 / 150keV) CT values, as shown in Table 5.

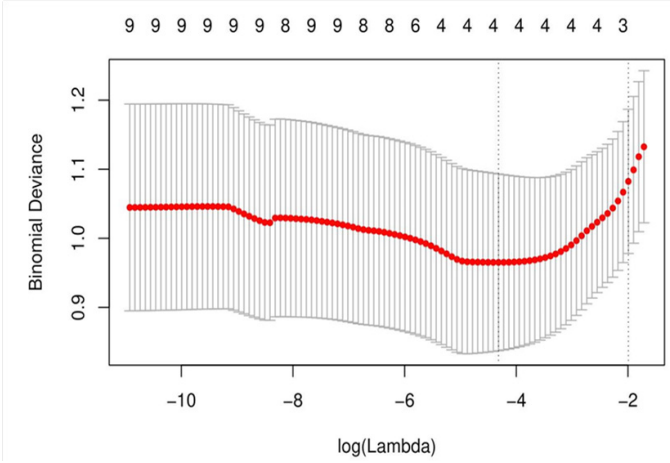

Figure 3: LASSO multivariate regression analysis.

Six clinical features and manual imaging features obtained by LASSO multivariate regression analysis were constructed as mixed clinical manual imaging models in the training set and then independently verified with the validation set.

Results of imaging omics analysis

The imaging omics features within ROI 1 and ROI 2 were extracted. The 63-dimensional features were obtained by predimension reduction (p<0.001) after univariate analysis. The LASSO multivariate regression analysis screened out the 10-dimensional features (p<0.05) highly related to the degree of lung adenocarcinoma invasion, and the imaging omics model was established, as shown in Figure 4 and Table 6.

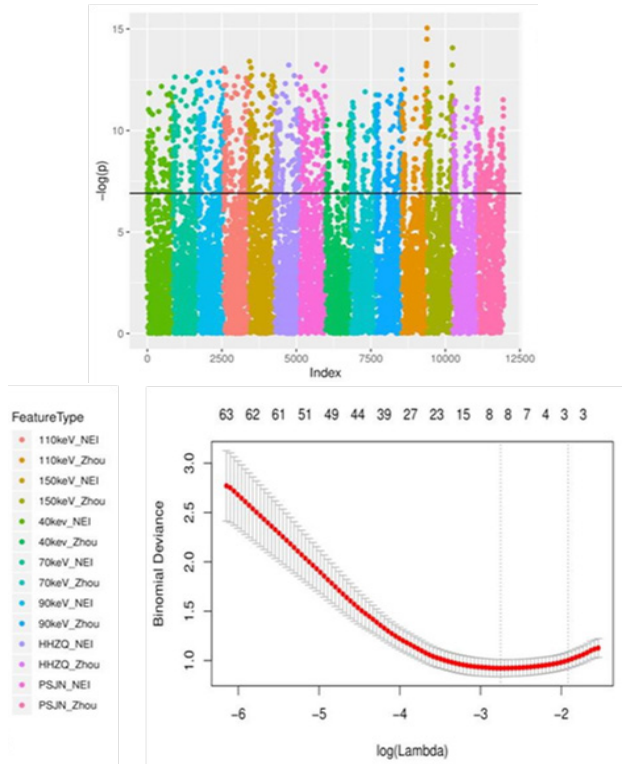

Figure 4: Manhattan diagram and LASSO dimensionality reduction map for univariate analysis of imaging omics characteristics.

Note: Figure A shows the results after univariate analysis of imaging omics characteristics and is shown in Manhattan diagram. A total of 63 features retain p <0.001 (above the black line in Fig). Figure B shows LASSO dimensionality reduction for 63 features with a total of 10 features with p <0.05.

Table 6: Imagiomics features of the included model after LASSO multivariate regression analysis.

Radiomics characteristics	Radiomic s group	Filter	coefficient	image sequence	ROI
Skewness	first order	wavelet. HLL	0.256198904	Non-contrast	2
Minimum	first order	wavelet.LHH	-0.006732907	Non-contrast	1
Gray Level Non Uniformity Normalized	glszm	wavelet. LLL	-0.291804896	Non-contrast	1
Maximum	first order	wavelet. LHL	0.010350669	Mixedenergy	1
Maximum	first order	wavelet. LHL	0.06352846	90keV	1
Size Zone Non Uniformity Normalized	glszm	wavelet. HLH	-0.195647523	90keV	1
Low Gray Level Zone Emphasis	glszm	wavelet. LHH	-0.28452662	70keV	2
Small Area Low Gray Level Emphasis	glszm	wavelet. LLL	-0.063355079	90keV	2
Small Area Low Gray Level Emphasis	glszm	wavelet. LLL	-0.27553465	110keV	2
Large Dependence Low Gray Level Emphasis	gldm	wavelet. LHH	-0.099725852	70keV	2

Establishment of the hybrid model

The imaging omics features after LASSSO dimension reduction were merged into the imaging omics scores, and then the statistically significant manual imaging features, clinical features and imaging omics scores were jointly constructed after multivariate analysis. In the process of establishing the mixed model, the quantitative characteristics such as the maximum diameter and CT value of all lesions were eliminated, so as to avoid duplication with the imaging omics characteristics and cause repeated measurements. In the mixed model, only the imaging-omics score (p=0.005) was an independent predictor of the degree of early lung adenocarcinoma infiltration.

Comparison of the three models and the construction of the normograph

To compare the diagnostic efficacy of imaging omics models, hybrid clinical manual imaging models and hybrid models, the imaging omics model had the highest diagnostic efficacy, followed by the mixed model, and finally, the mixed clinical manual imaging

model. The ROC of the three models is shown in Figure 5. There was a statistical difference between the imaging omics and hybrid, and hybrid clinical manual imaging models, but there was no statistical difference between the imaging omics and hybrid models, and the six-dimensional capability map of the three models is shown in Figure 6.

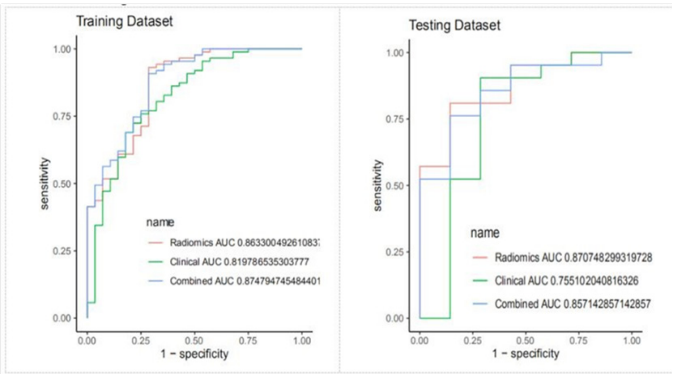

Figure 5: ROC curves of the 3 models in the training set and in the validation set.

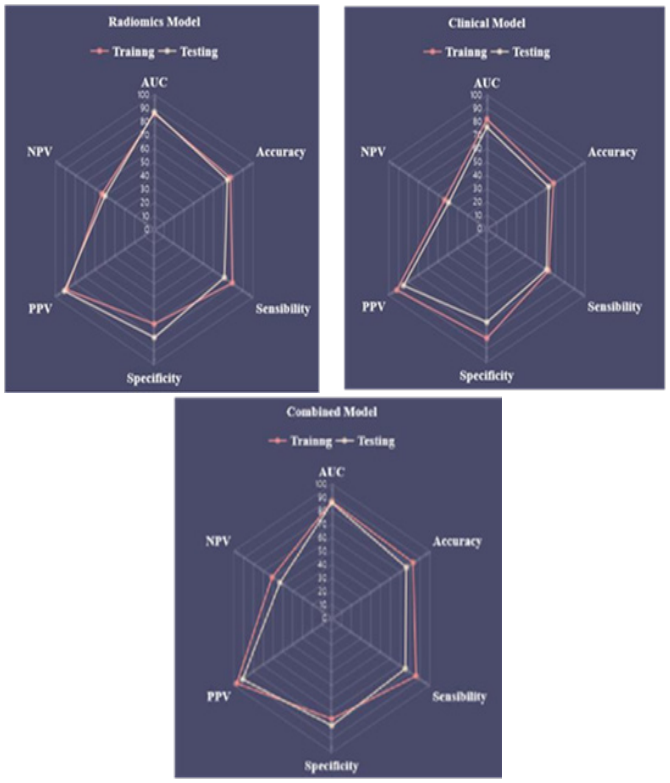

Figure 6: Six-dimensional capability diagram of the three models.

Discussion

The diagnostic value of CT on the extent of early lung adenocarcinoma

Some studies in the [2] affirmed the diagnostic value of MSCT and HRCT to determine the degree of pulmonary nodule infiltration, but it should be further verified by large sample size studies. With the advent of ESCT, some studies have shown that the detail display ability and diagnostic accuracy of ESCT for some pulmonary nodules are better than that of conventional CT [3]. Some studies [4,5] also show that the energy spectrum characteristics of pulmonary nodules combined with their morphological characteristics and some quantitative characteristics are conducive to the accurate diagnosis of pulmonary nodules infiltration degree.

Although the AUC value of the imaging omics model was slightly higher than that of the AUC value of the mixed model, there was no statistical difference in the diagnostic efficacy (DE LONG test p=0.84), and the accuracy, specificity and sensitivity of the mixed model were higher than that of the imaging model, so the mixed model was converted into norogram for clinical application, as shown in Figure 7.

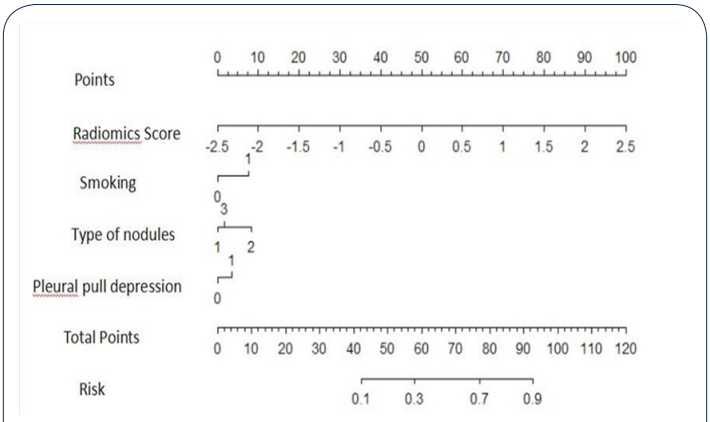

Figure 7: Norograph of the hybrid model.

The results of this study showed that the maximum diameter of the lesion, the plain scan CT value, and the single-energy imaging CT value in the enhanced scanning arterial period were all statistically significant. The mean size of the lesions in this group was 0.79 cm, 1.9 cm in the invasive group and 1.3 cm in the non-invasive group. The results of this study showed that the maximum lesion diameter was an independent risk factor for infiltration in early lung adenocarcinoma, which is consistent with previous literature findings in [6]. Some literature [7] suggested that lesion CT value was positively correlated with infiltration. In this study, the lesion CT values on single-energy imaging in the enhanced scanning arterial phase were statistically different between the two groups, which is consistent with previous studies on [8]. The study by Zhang et al. [9] showed that lesion CT values at higher energy levels (especially 140 keV) were an independent predictor of the degree of PGGN infiltration, with higher diagnostic accuracy in combination with lesion size. The results of this study show that the lesion enhanced CT value on single energy imaging is correlated with the degree of lesion infiltration, but multiple (40 / 90 / 150keV) levels are statistically significant, the reason is that the nodules included in this study, the best single energy levels of different types of nodules, leading to multiple lesions CT values on single energy imaging are statistically significant results. Due to the many types of nodules included in this study, the nodule size threshold and CT threshold were not analyzed in detail.

The nodule type, morphology and pleural traction depression in this study. Studies in [10] have pointed out that irregular shape or lobation is closely associated with the rapid appreciation of tumor cells, and that nodules with irregular shape or lobation usually predict a higher pathological grade. Another study [11]

showed that the nodule circularity predicted the longer-to-short diameter ratio and the leaf segmentation depth of PGGN infiltration more accurately. At present, most people believe that the pleural traction depression is mainly caused by the contraction of the fiber components in the lesion, and it is related to the location of the lesion (the lesion located in the subpleural area is more likely to appear in the pleural traction depression). The study by Chen et al [12] suggested that increased fibroblasts may be an early event in lung adenocarcinoma infiltration. In recent years, there is also a view that pleural pull depression may also be related to the infiltration of surrounding interstitial structures (lymphatic vessels, lobular space, pulmonary vessels, etc.), and some studies [13] shows that it is closely related to the degree of lung adenocarcinoma infiltration. However, the results of this study showed that the pleural pull depression was correlated with the degree of focal invasion, which was also consistent with the [14] results of some studies. The remaining qualitative features were not statistically different between the two groups. Among them, the lesion location, whether multiple nodules occurred, and air bronchial signs had no correlation with lung adenocarcinoma infiltration, which was consistent with most research findings of [15,16]. However, burr features, vacuoles, tumor-lung interface are clear, and vascular tract features are quite controversial. Some studies [17] showed that whether the burr sign and the tumor-lung interface are clear is correlated with the degree of lung adenocarcinoma infiltration, which is inconsistent with the results of this study. The reason is that the length of burr was not subdivided in this study. Long burr is usually considered to be correlated with inflammation, while short burr are mostly manifestations of focal infiltration. The vacuolar sign was not statistically different in this study, considering the influence of the included nodules type (the vacuolar sign mostly appeared in GGN, and the solid nodules were also included in the study may cause outcome bias). The literature reports that the vascular tract sign of [18] is an independent risk factor for invasive lung adenocarcinoma, Most of the previous studies have targeted a single type of nodules, However, the three types of nodules were included in this study, It may cause inconsistent research results; next, The vascular tract collection features included in this study included the traveling blood vessels in the GGN and the rectified or disrupted blood vessels in other types of nodules, The traveling blood vessels in GGN include blood vessels with obvious morphological changes, such as stenosis and distortion, and blood vessels with no obvious morphological changes, Crossing blood vessels without significant morphological changes may be normal pulmonary blood vessels, This study did not further distinguish between the morphological characteristics of the traveling blood vessels in the GGN, leading to possible errors in the results.

In the process of model construction, the maximum diameter and flat scan CT values were eliminated in multivariate analysis, considering the complex nodule types included in this study, and the maximum diameter and flat scan CT values of different types of nodules. In addition, the CT levels were low, medium and high, which were considered to be affected, but also suggested that energy spectrum CT can indeed provide richer and useful information. The mixed clinical manual imaging model of this study had the AUC values of the training set and the validation set of 0.82, and the accuracy of 0.68 and 0.63, respectively, which showed some diagnostic efficacy on the degree of infiltration of early lung adenocarcinoma. Xu et al. [19] also established three models to predict the degree of lung adenocarcinoma infiltration, respectively, the traditional feature model, imaging omics model and mixed model, AUC values of 0.824,0.833,0.848, the diagnostic efficacy of the traditional feature model is similar to the mixed clinical manual imaging model of this study, and the other two models are higher than the study model.

The diagnostic value of imaging model based on energy spectrum CT for the extent of early lung adenocarcinoma

In this study, 10 selected imaging omics features include the wavelet algorithm after filtering part of the first order features and texture features, specific analysis is as follows: (1) FIRSTORDER four imaging omics features: the skewness from different image sequence, maximum and minimum features filtered by the wavelet algorithm, these features are closely related to the uniformity of ROI. (2) Five imaging omics features from GLSZM and one imaging omics feature from GLDM: gray scale, size uniformity and low gray scale features from different image sequences filtered by wavelet algorithm. The inhomogeneity of gray scale and the non-uniformity of size area indicate that the volume variability of gray scale level and size area is closely related to the heterogeneity of ROI heterogeneity. The above features indicate that the uniformity and heterogeneity of IAC lesions are quite different from the pre-invasive lesions.

This study found that the 10 characteristics from the nodule itself and the proportion of the characteristics of the peritumoral microenvironment were consistent, suggesting that the peritumoral microenvironment also contains a lot of information related to the lesions. The peritumoral microenvironment characteristics obtained in this study mainly include deviation and gray characteristics, reflects the heterogeneity and uniformity of peritumoral microenvironment, which is closely related to the density of tumor infiltration lymphocytes in the tumor microenvironment, and the characteristics of [20] and lung adenocarcinoma infiltration degree [21], but the tumor microenvironment related research, is still in its infancy, more studies are needed to further confirm. In addition, this study also found that six of the 10 features came from single-energy imaging (including 70 keV, 90 keV, 110 keV). Although this level was not completely consistent with the statistically different manual feature level, it also verified the importance of energy spectrum CT for early lung adenocarcinoma infiltration degree discrimination, and the incomplete consistency of imaging features and manual imaging feature results resulted from manual measurement, so this information needs to be further mined and verified.

The imaging omics model of this study, combined with the imaging omics features of the lesion itself and in the peritumoral microenvironment, showed high AUC values (0.88,0.87) and accuracy (0.83,0.76) in the training set and validation set. Wu et al. [22] also studied the infiltration degree of lung adenocarcinoma, they also extracted the imaging omics characteristics of the nodules themselves and the peritumoral microenvironment and established a prediction model. The AUC value (training set AUC 0.89; the validation set AUC 0.87) was similar to the AUC value of this model, but the study object was pure ground glass nodules, highly targeted and higher diagnostic efficacy, which confirmed that CT can provide more useful information than conventional

CT. Yang et al. [23] study also included three types of lung nodules, but this study only extracted the imaging omics characteristics of lung nodules themselves and established the imaging omics model. The training set AUC value was 0.83; the validation set AUC value was 0.77, and the diagnostic efficacy was worse than that of the study model, which shows that the imaging omics characteristics in the peritumoral microenvironment do help to improve the ability of the imaging omics model to predict the degree of early lung adenocarcinoma infiltration.

Clinical features, CT morphological features and imaging omics score were combined. The AUC values in the training set were 0.87 and 0.86, respectively; the accuracy was 0.83 and 0.76, respectively. The results of this study showed that only the imaging omics score in the mixed model was an independent predictor of the infiltration extent of early lung adenocarcinoma. Xue et al. [24] determined the degree of infiltration of 599 PGGN by combining morphological characteristics and imaging omics characteristics. The AUC values of training and validation groups were 0.76 and 0.79 respectively. In addition, the diagnostic efficacy of the imaging omics model and mixed model (AUC value established by Xu et al. [25] was 0.833 and 0.848 respectively) was not good to the imaging omics model and mixed model in this study. The reason is that this study used DECT scan and extracted the imaging features within the peritumoral microenvironment, dug out more information helpful to identify the infiltration degree of lung adenocarcinoma invasion, and improved the diagnostic efficacy of the study model. She et al. [26] distinguished the pre-invasive (AAH / A I S/MIA) and invasive (IAC) lesions from 402 nodules and established a diagnostic model. The AUC value (0.96 and 0.90, respectively) was higher than the mixed model of this study because of the small sample size of this study, especially the large sample size difference between the pre-invasive lesions and invasive lesions, which ultimately led to the weak diagnostic efficacy of the study model.

The results of this study showed that the AUC value and diagnostic accuracy of imaging omics model and mixed model were higher than those of mixed clinical manual imaging model, and the difference was statistically significant. Some and only the imaging omics score were the independent predictors of the invasion degree of early lung adenocarcinoma in the model. The observation and measurement of manual imaging features were limited to the naked eye and related to the observer experience, with large error. However, the extraction of the imaging omics features is more unified and comprehensive, the lesion analysis is more sufficient, and the judgment of the lesion infiltration is more accurate. However, the processing of imaging omics data is more complex and requires professional software, so it is still not widely used in clinical practice.

This study has the following limitations: First, the sample size of this study is only 196 cases, and the research content is more, which affects the sensitivity and specificity of the model to some extent. Second, three types of pulmonary nodules were included in this study and were not analyzed for a single type of pulmonary nodules, which may bias the analysis of some manual imaging features. Third, this study was a single-center, single-image source, and did not include CT images of the chest energy spectrum except for FORCE CT, so the model applicability was limited.

References

1. Sung H, Ferlay J, Siegel R L, Laversanne M, Soerjomataram I et al. Global Cancer Statistics 2020: GLOBOCAN Estimates of Incidence and Mortality Worldwide for 36 Cancers in 185 Countries. CA Cancer J Clin. 2021; 71: 209-249.
2. Li FH. Analysis of 64 slice spiral CT dynamic enhanced scanning characteristics of solitary pulmonary nodules in patients with lung cancer of different pathological types. Journal of Taishan Medical College. 2020; 41: 913-915.
3. Li Q, Tan H, Lv F. Molecular characterization of solitary pulmonary nodules in dual-energy CT nonlinear image fusion technology. J Recept Signal Transduct Res. 2020: 1-5.
4. Meng PW, Wang HL, Liu L, et al. Study on the value of force CT energy spectrum purification technology in the evaluation of pulmonary ground glass nodules. Journal of Medical Imaging. 2020; 30: 960-964.
5. Wang YL, Xiang SH, Li N, et al. Value of quantitative parameters of energy spectrum CT in qualitative diagnosis of pulmonary ground glass nodules. Tumor. 2020; 40: 488-495.
6. Zhou QJ, Zheng ZC, Zhu YQ, et al. Tumor invasiveness defined by IASLC/ATS/ERS classification of ground-glass nodules can be predicted by quantitative CT parameters. J Thorac Dis. 2017; 9: 1190-1200.
7. Tan XM. Value of dual source CT dual energy imaging in differential diagnosis of preinvasive lesions \ microinvasive adenocarcinoma and invasive adenocarcinoma presenting as pulmonary nodules, Guangxi Medical University, 2019.
8. Yang Y, Li K, Sun D, Yu J, Cai1 Z, et al. Invasive Pulmonary Adenocarcinomas Versus Preinvasive Lesions Appearing as Pure Ground-Glass Nodules: Differentiation Using Enhanced Dual-Source Dual-Energy CT. AJR Am J Roentgenol. 2019; 213: W114-W122.
9. Zhang Y, Tang J, Xu J, Cheng J, Wu H et al. Analysis of pulmonary pure ground-glass nodule in enhanced dual energy CT imaging for predicting invasive adenocarcinoma: comparing with conventional thin-section CT imaging. J Thorac Dis, 2017; 9: 4967-4978.
10. Ding H, Shi J, Zhou X, Xie D, Song X, et al. Value of CT Characteristics in Predicting Invasiveness of Adenocarcinoma Presented as Pulmonary Ground-Glass Nodules. Thorac Cardiovasc Surg. 2017; 65: 136-141.
11. Ba W J, Xu D, Yin K. HRCT signs evaluate the infiltration of pure ground glass nodules: the roundness of pulmonary nodules is better than the long short diameter ratio and the lobulation depth. Radiology practice. 2020; 35: 1542-1546.
12. Chen C, Li WJ, Weng JJ, Chen Z-J, Wen Y-Y, et al. Cancer-associated fibroblasts, matrix metalloproteinase-9 and lymphatic vessel density are associated with progression from adenocarcinoma in situ to invasive adenocarcinoma of the lung. Oncol Lett. 2020; 20: 130.
13. Fang Rui. Analysis of factors related to pleural depression sign and visceral pleural invasion of pure ground glass density nodules within 10mm from the pleura in lung adenocarcinoma PLA Medical College, 2019.
14. Qiu ZX, Li WM. Analysis of clinical, pathological and imaging features of 328 cases of lung cancer with solitary ground glass nodules on HRCT. Chinese Journal of respiratory and critical care. 2018; 17: 470-476.

15. Jin X, Zhao S H, Gao J, et al. CT characteristics and pathological implications of early stage (T1N0M0) lung adenocarcinoma wit pure ground-glass opacity. Eur Radiol. 2015; 25: 2532-2540.

16. Silva M, Bankier AA, Centra F, Colombi D, Ampollini L, et al. Longitudinal evolution of incidentally detected solitary pure ground-glass nodules on CT: relation to clinical metrics. Diagn Interv Radiol. 2015; 21: 385-390.

17. Xing Y, Li Z, Jiang S, Xiang W, Sun X, et al. Analysis of pre-invasive lung adenocarcinoma lesions on thin-section computerized tomography. Clin Respir J. 2015; 9: 289-296.

18. Lu J, Tang H, Yang X, Liu L, Pang M, et al. Diagnostic value and imaging features of multi-detector CT in lung adenocarcinoma with ground glass nodule patients. Oncol Lett. 2020; 20: 693-698.

19. Xu F, Zhu W, Shen Y, Wang J, Xu R, et al. Radiomic-Based Quantitative CT Analysis of Pure Ground-Glass Nodules to Predict the Invasiveness of Lung Adenocarcinoma. Front Oncol. 2020; 10: 872.

20. Koh YW, Jeon YK, Yoon DH, Suh C, Huh J, et al. Programmed death 1 expression in the peritumoral microenvironment is associated with a poorer prognosis in classical Hodgkin lymphoma. Tumour Biol. 2016; 37: 7507-7514.

21. Beig N, Khorrami M, Alilou M, Prasanna P, Braman N, et al. Perinodular and Intranodular Radiomic Features on Lung CT Images Distinguish Adenocarcinomas from Granulomas. Radiology. 2019; 290: 783-792.

22. Wu L, Gao C, Xiang P, Zheng S, Pang P, et al. CT-Imaging Based Analysis of Invasive Lung Adenocarcinoma Presenting as Ground Glass Nodules Using Peri- and Intra-nodular Radiomic Features. Front Oncol. 2020;10: 838.

23. Yang B, Guo L, Lu G, Shan W, Duan L, et al. Radiomic signature: a non-invasive biomarker for discriminating invasive and non-invasive cases of lung adenocarcinoma. Cancer Manag Res. 2019; 11: 7825-7834.

24. Xue X, Yang Y, Huang Q, Cui F, Lian Y, et al. Use of a Radiomics Model to Predict Tumor Invasiveness of Pulmonary Adenocarcinomas Appearing as Pulmonary Ground-Glass Nodules. Biomed Res Int. 2018; 2018: 6803971.

25. Xu F, Zhu W, Shen Y, Wang J, Xu R, et al. Radiomic-Based Quantitative CT Analysis of Pure Ground-Glass Nodules to Predict the Invasiveness of Lung Adenocarcinoma. Front Oncol. 2020; 10: 872.

26. She Y, Zhang L, Zhu H, Dai C, Xie D, et al. The predictive value of CT-based radiomics in differentiating indolent from invasive lung adenocarcinoma in patients with pulmonary nodules. Eur Radiol. 2018; 28: 5121-5128.